Magnetization Reversal of Nanoscale Islands: How Size and Shape Affect the Arrhenius Prefactor

S. Krause,[1,*] G. Herzog,[1] T. Stapelfeldt,[1] L. Berbil-Bautista,[1,†] M. Bode,[1,‡] E. Y. Vedmedenko,[1] and R. Wiesendanger[1]

[1]*Institute of Applied Physics and Microstructure Research Center, University of Hamburg,
Jungiusstrasse 11, 20355 Hamburg, Germany*
(Received 7 July 2009; published 14 September 2009)

The thermal switching behavior of individual in-plane magnetized Fe/W(110) nanoislands is investigated by a combined study of variable-temperature spin-polarized scanning tunneling microscopy and Monte Carlo simulations. Even for islands consisting of less than 100 atoms the magnetization reversal takes place via nucleation and propagation. The Arrhenius prefactor is found to strongly depend on the individual island size and shape, and based on the experimental results a simple model is developed to describe the magnetization reversal in terms of metastable states. Complementary Monte Carlo simulations confirm the model and provide new insight into the microscopic processes involved in magnetization reversal of smallest nanomagnets.

The vast growth of storage density in magnetic media is closely connected to the miniaturization of bit size. Below a critical size, however, thermal agitation leads to a magnetization reversal of the grains that represent a bit, thereby destroying stored information. Therefore it is highly relevant to understand the underlying physical processes that favor or hinder magnetization reversal inside a nanomagnet.

In early theoretical approaches Néel [1] and Brown [2] calculated the switching probability for monodomain particles of uniaxial anisotropy. The mean lifetime $\bar{\tau}$ between consecutive switching events of a particle as a function of temperature T is characterized by its activation barrier E_b and attempt frequency ν_0,

$$\bar{\tau} = \nu_0^{-1} \exp\left(\frac{E_b}{k_B T}\right), \qquad (1)$$

with k_B being the Boltzmann constant. In this model, magnetization reversal is realized by a coherent rotation of all magnetic moments inside the particle, with E_b given by the total magnetic anisotropy of the particle. The prefactor ν_0 is commonly related to Larmor precession, with $\nu_0 \approx 10^{10}$ Hz [2].

Depending on the magnetic anisotropy, exchange parameter and size, a monodomain particle may reverse its magnetization via nucleation and propagation rather than by a coherent rotation. Like in the Néel-Brown model, an Arrhenius-like switching behavior is expected, now with E_b represented by the energy needed for the combined nucleation and domain wall formation. Whereas there are many studies focusing on the details of the energy barrier E_b and the microscopic processes for magnetization reversal, the fundamental physics of the prefactor ν_0 is not revealed. In general, ν_0 is considered to be a constant which only depends on material properties of the system, but size or shape effects have been neglected. A detailed study on the Arrhenius prefactor of nanomagnets that reverse their magnetization via nucleation and diffusion

was lacking up to now, because laterally and time-averaging experimental techniques are not suitable to investigate the switching behavior of individual atomic-scale nano-objects. However, spin-polarized scanning tunneling microscopy (SP-STM) serves as a unique tool to directly probe the magnetization of individual nanoislands.

Our studies using combined temperature-dependent SP-STM experiments and Monte Carlo (MC) simulations reveal that monolayer iron islands on W(110) consisting of 30 atoms and more reverse their magnetization via the nucleation and propagation of a domain wall, whereas we have indications that for islands consisting of less than 30 atoms the reversal takes place via a coherent rotation of the magnetic moments. Although an Arrhenius-like switching has been observed, both the experimental and the theoretical investigations show that ν_0 strongly depends on the size and the shape of the nanoislands—which is not expected within the Néel-Brown model.

The experimental investigations were performed in an ultrahigh vacuum system that is equipped with a homebuilt spin-polarized scanning tunneling microscope for variable temperatures. Within our experimental setup, the entire microscope including the tip is cooled to minimize the thermal drift between tip and sample. While staying in tunneling contact, the temperature can be varied by more than 10 K without the nanoisland that is to be investigated drifting out of the tip scan range. The base pressure in both the preparation and the STM chamber is in the low 10^{-11} torr range. To exclude any unwanted dipolar tip-sample interaction, antiferromagnetic Cr coated tips were used that are sensitive to the in-plane component of the sample magnetization [3,4].

A W(110) single crystal serves as substrate for our experiments. Its preparation is described in detail in Ref. [5]. Evaporating 0.14 atomic layers of iron onto the substrate held at room temperature leads to the formation of pseudomorphically grown nanoislands which have a typical diameter between 2 and 6 nm, thereby consisting

of about 30–150 atoms. The thermal switching behavior of 11 nanoislands that differ in size and shape has been investigated in detail as a function of temperature. A topography patchwork of the nanoislands is shown in Fig. 1(a). All experiments have been performed at temperatures between $T = 30$ K and $T = 80$ K. The magnetic probe tip has been positioned on top of the center of an individual island to record the temporal evolution of the differential conductance dI/dU, measured by adding a small ac modulation voltage ($U_{mod} = 40$ mV) to the sample bias and detecting the resulting modulation of the tunneling current I by lock-in technique. The spin-dependent contribution to the dI/dU signal scales with $\cos\alpha$, where α is the angle between the magnetization directions of the tip and sample [4].

In Fig. 1(b) a section of the telegraphic $dI/dU(t)$ signal is exemplarily shown for nanoisland "9" at a fixed temperature $T = 53.6$ K. The signal abruptly changes between two discrete levels, reflecting the island magnetization
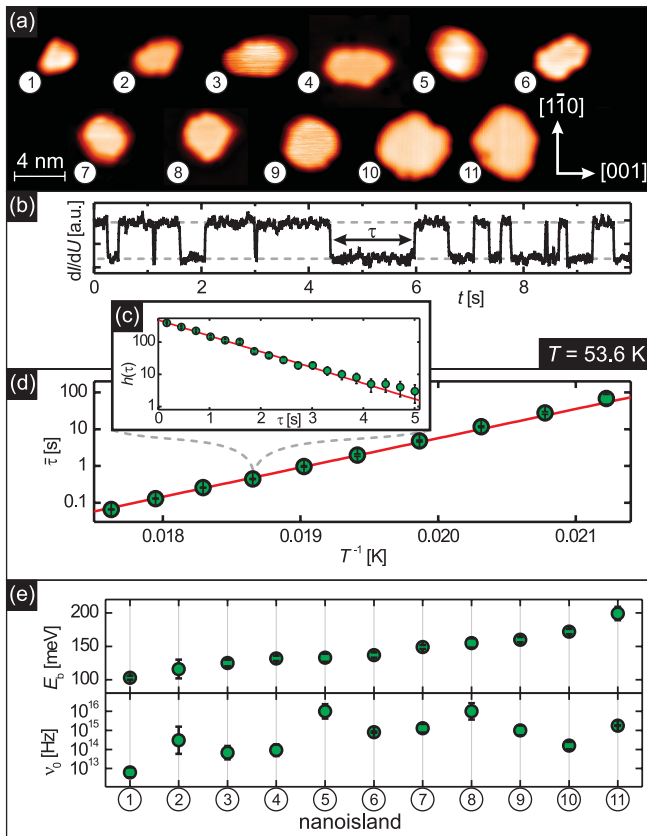

FIG. 1 (color). (a) Topography maps of all nanoislands investigated. (b) Section of the magnetic $dI/dU(t)$ signal as recorded above the center of an individual island. Every lifetime τ in between two consecutive switching events has been determined (see arrow). (c) Respective histogram $h(\tau)$ of the lifetimes τ. Fitting with a decay law results in the mean lifetime $\bar{\tau}$. (d) Mean lifetime $\bar{\tau}(T^{-1})$ as determined for different temperatures T. (e) Effective activation energy barrier E_b (top panel) and prefactor ν_0 (bottom panel) as determined for each of the nanoislands.

switching between two configurations with respect to the stable tip magnetization. From earlier investigations on the Fe/W(110) system it is known that the monolayer exhibits a uniaxial anistropy with an easy axis of magnetization oriented along the $[1\bar{1}0]$ direction [6,7], which is in consistence with our observation. Plotting the histogram $h(\tau)$ of all the lifetimes τ between consecutive switching events, as shown in Fig. 1(c), reveals that the lifetime distribution can be described by an exponential decay law, and fitting the data results in the mean lifetime $\bar{\tau}(T)$. Approximately 1000 switching events have been recorded to assure good statistics on the lifetime distribution. This procedure of mean lifetime determination was repeated at different temperatures on the same nanoisland. The result for the exemplary nanoisland is shown in Fig. 1(d). An Arrhenius-like behavior of $\bar{\tau}(T^{-1})$ is clearly visible; therefore, it is reasonable to fit the data with Eq. (1), yielding the effective activation energy barrier E_b and the prefactor ν_0. The respective fitting parameters E_b and ν_0 for all investigated nanoislands are summarized in Fig. 1(e). Note that ν_0 is on the order of 10^{13} and 10^{16} Hz, whereas the observed switching frequencies are on the order of Hz—hence, the observed magnetization reversals are very rare events.

In Fig. 2(a), E_b is plotted as a function of the respective island length along the $[1\bar{1}0]$ direction, $N_{[1\bar{1}0]}$, counted in atomic rows (AR). Obviously, E_b scales linearly with
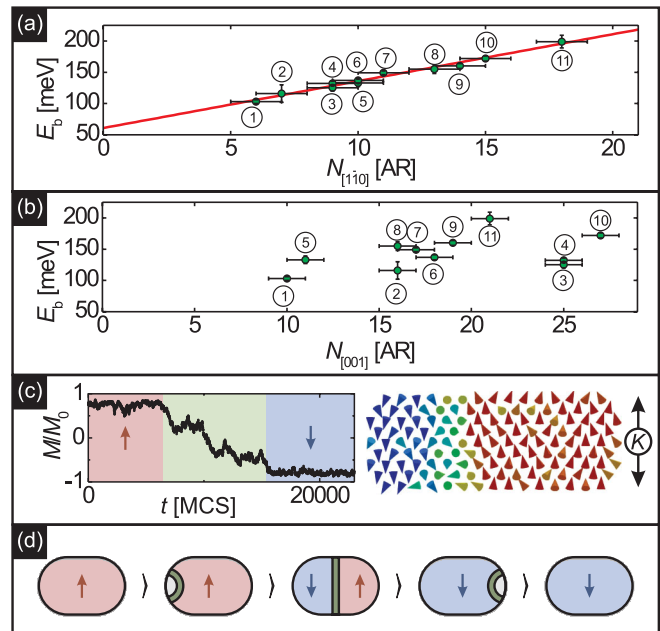

FIG. 2 (color). Activation energy barrier E_b plotted as a function of length N of the nanoisland along (a) the $[1\bar{1}0]$ direction and (b) the [001] direction. (c) Monte Carlo simulation: Evolution of the island magnetization M (M_0: saturation magnetization) for a typical switching event (left panel). Snapshot of the spin-configuration during reversal (right). Every cone represents one magnetic moment, while the color scheme denotes the orientation. (d) Model of magnetization reversal via nucleation and propagation of a domain wall.

$N_{[1\bar{1}0]}$, whereas no clear dependence on the length along the [001] direction $N_{[001]}$ is visible, as can be seen in Fig. 2(b). The clear linear scaling behavior with $N_{[1\bar{1}0]}$ in Fig. 2(a) indicates that reversal takes place via the nucleation and propagation of a domain wall that aligns along the $[1\bar{1}0]$ direction and consequently moves along the [001] direction. As $N_{[1\bar{1}0]}$ increases, the respective length of the domain wall (and therefore its energy) increases accordingly. Fitting the experimentally obtained activation energy barriers $E_b(N_{[1\bar{1}0]})$ in Fig. 2(a) to a linear function of the type

$$E_b(N_{[1\bar{1}0]}) = E_0 + e_{DW}N_{[1\bar{1}0]} \qquad (2)$$

results in $E_0 = (61 \pm 5)$ meV and $e_{DW} = (7.5 \pm 0.4)$ meV/AR. The energy offset E_0 includes rim effects as well as the energy for the creation of a reversed nucleus [8]. Within additional investigations on the Fe/W(110) closed monolayer system the domain wall width has been found to be $w = (2.15 \pm 0.35)$ nm [8]. Using e_{DW} and w, the uniaxial anisotropy in the $[1\bar{1}0]$ direction, $K = (0.55 \pm 0.03)$ meV/atom, and the exchange stiffness component in the [001] direction, $A_{[001]} = (9.07 \pm 0.42)$ meV, have been derived [8].

Hence, two important issues have been experimentally revealed: a nonvanishing offset in the activation energy and an orientational preference of the domain walls. While similar effects have been discussed in the literature with respect to ground states of ultrathin films [9,10] and quasi-static magnetization reversal [11], their role for the thermally induced switching behavior is unknown so far. To shed light on this important issue, MC simulations of thermal activated magnetization reversal in Fe/W(110) monolayer islands have been performed for different island sizes and shapes, using the experimentally determined parameters $A_{[001]}$ and K. For the calculations the procedure described in [9] has been used, with the exchange interactions along the $[1\bar{1}0]$ direction taken to be twice as strong as those along the [001] direction, according to previous investigations [9,10].

A typical switching event as calculated within the MC simulations is shown in Fig. 2(c). In contrast to the SP-STM experiment, the detailed magnetization reversal processes can be resolved at any given simulation time t. The snapshot in the right panel of Fig. 2(c) shows the magnetic configuration of the simulated island during reversal. It is clearly visible that a domain wall separates a spin-up domain from a spin-down domain. Composing a movie from many consecutive snapshots reveals that the domain wall propagates from one end of the island to the other, thereby leading to a reversal of the magnetization [8]. Because of the strong anisotropy of the exchange stiffness tensor the domain walls have been found to be mainly oriented along the $[1\bar{1}0]$ axis independently of the sample shape. Because of this anisotropy, E_b scales linearly with $N_{[1\bar{1}0]}$, but does not depend on $N_{[001]}$. The detailed analysis of numerous switching events has shown that the magne-

tization reversal usually starts at one of the [001] ends of an island, whereas nucleation events taking place far away from the [001] ends are very rare. Consequently, the simulations support the experimental finding of temperature induced magnetization reversal via nucleation and propagation.

In Fig. 2(d), a detailed model for the magnetization reversal is developed. Initially, the island is in a monodomain state. The reversal starts by the coherent rotation of several magnetic moments within a small nucleus. This nucleus is confined by a domain wall that propagates along the [001] direction through the whole nanoisland with Boltzmann probability. Only a domain wall propagation from one end of the island to the other leads to a net magnetization reversal of the nanoisland, whereas the initial magnetic configuration is restored if the domain wall annihilates at the nucleation site.

The exciting question arises on how the size and shape of a nanoisland affects its switching rate. In Fig. 3(a), the experimentally determined prefactor ν_0 is plotted as a function of $N_{[001]}$ and $N_{[1\bar{1}0]}$. Adding a contour plot to the graph reveals that all data points (apart from the smallest
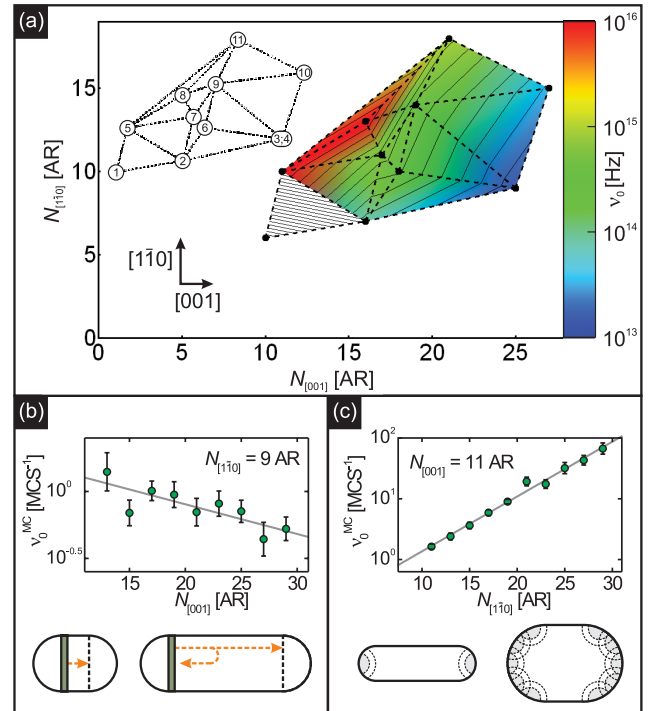

FIG. 3 (color). (a) Experimentally determined prefactor ν_0 as a function of island length $N_{[1\bar{1}0]}$ and $N_{[001]}$. See labeled mesh inset for island correlation. (b) Prefactor $\nu_0^{MC}(N_{[001]})$ from Monte Carlo simulations for $N_{[1\bar{1}0]} = 9$ AR. A tendency of decreasing ν_0^{MC} with increasing $N_{[001]}$ is clearly visible. (c) Prefactor $\nu_0^{MC}(N_{[1\bar{1}0]})$ from Monte Carlo simulations for $N_{[001]} = 11$ AR, revealing that ν_0^{MC} increases with increasing $N_{[1\bar{1}0]}$. Note that ν_0^{MC} is given in units of MCS^{-1}, whereas ν_0 is given in units of Hz. The lines within the graphs are guides for the eyes.

nanoisland, labeled "1") seem to lie on a plane in the three-dimensional ($N_{[001]}$, $N_{[1\bar{1}0]}$, $\log_{10}[\nu_0/\nu_{\text{unit}}]$) space ($\nu_{\text{unit}} = 1$ Hz), as indicated by the interpolated color gradient ranging from high ν_0 values (red) on the upper left to low values (blue) on the lower right of the graph. The prefactor ν_0 of the smallest island considerably deviates from this scheme. We speculate that—due to its small size—this island reverses its magnetization via a coherent rotation of the magnetic moments rather than by a nucleation and propagation. The activation energy barrier E_b has been used to elaborate rim effects, resulting in the anisotropy of rim atoms $K_{\text{rim}} \approx 5.6$ meV/atom [8]. Figure 3(a) shows that ν_0 should increase when increasing $N_{[1\bar{1}0]}$ while keeping $N_{[001]}$ constant, whereas ν_0 should decrease when increasing $N_{[001]}$ while keeping $N_{[1\bar{1}0]}$ constant.

In order to check this statement on a theoretical basis we performed MC simulations for islands of fixed $N_{[1\bar{1}0]}$ ($N_{[001]}$) while changing $N_{[001]}$ ($N_{[1\bar{1}0]}$), respectively. For every island, the telegraphic signal of the magnetization $M(t)$ [t given by the Monte Carlo steps (MCS)] has been calculated for different temperatures T, resulting in numerous switching events. For every temperature, $M(t)$ has been analyzed in terms of switching frequency ν^{MC} (analog to the experimental data). An Arrhenius-like behavior is observed, and fitting the Néel-Brown model yields the activation energy barrier E_b^{MC} and the prefactor ν_0^{MC} of the respective simulated nanoisland. In Fig. 3(b), $\nu_0^{\text{MC}}(N_{[001]})$ is shown for a fixed $N_{[1\bar{1}0]}$, revealing that ν_0^{MC} decreases with increasing $N_{[001]}$. In Fig. 3(c), $\nu_0^{\text{MC}}(N_{[1\bar{1}0]})$ is shown for a fixed $N_{[001]}$. Here, ν_0^{MC} increases with increasing $N_{[1\bar{1}0]}$. Obviously, the simulations are in qualitative agreement with the experimental data.

The experimental as well as the simulation results can be understood in the framework of the following simple model. After the nucleation the domain wall can be described as a quasiparticle propagating through the nanoisland. Because of the absence of external forces (note that in our experiments no external magnetic field is applied), moving forward and backward is energetically degenerate. Following random walk theory for a particle moving along a line with absorbing ends [12], the mean distance covered after n steps scales with $\sqrt{n}$. Thus, the probability of a domain wall successfully propagating from one end of the island to the other decreases with increasing $N_{[001]}$, as depicted in Fig. 3(b). For very elongated islands it is likely that the domain wall returns to its nucleation site and annihilates there, with no net magnetization reversal. This behavior is reflected by the decrease of ν_0 when increasing $N_{[001]}$ and keeping $N_{[1\bar{1}0]}$ constant. With increasing $N_{[1\bar{1}0]}$, the number of nucleation sites for magnetization reversal increases. Thus, every additional nucleation center increases the probability of magnetization reversal.

Consequently, ν_0 increases when increasing $N_{[1\bar{1}0]}$ while keeping $N_{[001]}$ constant. Therefore, the prefactor ν_0 is determined by the probability of a domain wall to propagate through the whole nanoisland and the number of nucleation sites.

In summary, we performed a combined experimental and theoretical study on the thermally induced magnetization reversal of atomic-scale monolayer iron nanoislands, thereby providing insight into the microscopic processes of magnetization reversal. Even very small nano-objects consisting of only a few atoms may switch their magnetization by nucleation and propagation. The Arrhenius prefactor is found to be strongly dependent on the morphology of each individual object: Tiny differences in size or shape can lead to a variation of the switching rate by orders of magnitude. Our studies help to systematically tailor future magnetic nano-objects that hinder or favor magnetization reversal, which is important for the development of new types of data storage media or magnetic sensors at the nanoscale.

*skrause@physnet.uni-hamburg.de
†Present address: Materials Sciences Division, Lawrence Berkeley National Laboratory, Berkeley, CA 94720, USA.
‡Present address: Center for Nanoscale Materials, Argonne National Laboratory, Argonne, IL 60439, USA.

[1] M. L. Néel, Ann. Geophys. **5**, 99 (1949).
[2] W. F. Brown, Phys. Rev. **130**, 1677 (1963).
[3] A. Kubetzka, M. Bode, O. Pietzsch, and R. Wiesendanger, Phys. Rev. Lett. **88**, 057201 (2002).
[4] A. Wachowiak, J. Wiebe, M. Bode, O. Pietzsch, M. Morgenstern, and R. Wiesendanger, Science **298**, 577 (2002).
[5] M. Bode, S. Krause, L. Berbil-Bautista, S. Heinze, and R. Wiesendanger, Surf. Sci. **601**, 3308 (2007).
[6] M. Pratzer, H. J. Elmers, M. Bode, O. Pietzsch, A. Kubetzka, and R. Wiesendanger, Phys. Rev. Lett. **87**, 127201 (2001).
[7] M. Pratzer and H. J. Elmers, Phys. Rev. B **67**, 094416 (2003).
[8] See EPAPS Document No. E-PRLTAO-103-069938 for supplementary material. For more information on EPAPS, see http://www.aip.org/pubservs/epaps.html.
[9] E. Y. Vedmedenko, A. Kubetzka, K. von Bergmann, O. Pietzsch, M. Bode, J. Kirschner, H. P. Oepen, and R. Wiesendanger, Phys. Rev. Lett. **92**, 077207 (2004).
[10] R. B. Muniz, A. T. Costa, and D. L. Mills, J. Phys. Condens. Matter **15**, S495 (2003).
[11] J. Vogel, J. Moritz, and O. Fruchart, C.R. Physique **7**, 977 (2006).
[12] G. Ehrlich, J. Chem. Phys. **44**, 1050 (1966).